

Synthesis, Characterization and Anticancer Activity of Pyrazine-2-Carboxamide Metal Complexes

¹Mohsin Ali, ²Zi-Ning Lei, ³Mansoor Ahmed*, ⁴Syed Imran Ali, ²Konatsu Kojima, ²Pranav Gupta, ¹Majid Mumtaz, ²Zhe-Sheng Chen, ⁵Syed Moazzam Haider, ³Muhammad Hanif, ³Ameer Hassan and ²Dong-Hua Yang

¹Department of Chemistry, University of Karachi, Karachi-75270, Pakistan.

²Department of Pharmaceutical Sciences, College of Pharmacy and Health Sciences, St. John's University, Queens, NY 11439, USA)

³Department of Pharmaceutical Chemistry, University of Karachi, Karachi-75270, Pakistan)

⁴Department of Applied Chemistry & Chemical Technology, University of Karachi, Karachi-75270, Pakistan

⁵Industrial Analytical Center (ICCBS), University of Karachi, Karachi-75270, Pakistan)

mohsin.ali@uok.edu.pk, cando@cyber.net.pk*

(Received on 22nd November 2017, accepted in revised form 25th June 2018)

Summary: We explore the synthesis of metal complexes of a renowned antituberculosis drug, pyrazinamide (PZ) with copper, ferrous, ferric, cobalt and manganese. A detailed characterization of the resulting complexes was performed for establishing their structures by using spectroscopic techniques like NMR, FTIR, PXRD and SEM. These compounds were also explored for anticancer activity on SNB-19, HCT-15, COLO-205, and KB-3-1 cell lines and were found to be non-or low toxicity as most of the tested compounds' IC₅₀ > 100 µM. Scanning electron microscopy (SEM) revealed marked changes in the morphology after complexation. Compared to the pure PZ, an abrupt change in the morphological features of the complexes was likely caused by the chelating of PZ molecules with the metals. The micrographs of complexes depict a uniform matrix which indicates complete complex formation of with the drug uniformly dispersed at the molecular level. X-ray diffraction (PXRD) data suggested crystalline nature for the pure ligand and its corresponding complexes and this observation is well supported by morphological characterizations performed using Scanning Electron Microscopy.

Keywords: Drug Metal Complexes, Pyrazinamide, Scanning Electron Microscopy, X-Ray Diffraction Cytotoxicity, Spectroscopic investigation.

Introduction

Agents related to hetero aromatic class of substances are of high significance in drug discovery studies owing to their wide availability in multiple drugs used for treating different ailments. Pyrazine, a member of this class of substances, is found in natural compounds as well as in many drugs showing multiple biological activities [1], examples include Gliplizide, an oral hypoglycemic agent [2]. Pyrazinamide (PZ) has been used over the years as the first and second line anti-tuberculosis agent [3], Telaprevir agent for treating Hepatitis C [4], Oltiprazm, a schistosomicidal and tumor preventing agent [5, 6] and Bortezomib, used against Multiple Myeloma [7, 8].

The fields of coordination and material chemistry have produced novel coordination polymers of practicable importance in the sectors of adsorption science and catalysis [9-14]. Metal complexes bearing PZ as a ligand have been demonstrated to possess improved anti-mycobacterial properties [15]. PZ can coordinate through the pyrazine ring nitrogen and its strong hydrogen

bonding ability along with its ability to act as ligand in multiple complexes with transition metals makes it a potential candidate for the synthesis of various highly organized and distinct coordination polymers [16-19].

Copper plays a crucial role in different biological systems as a part of enzymes and proteins. Reported research has revealed various copper complexes with anti-amoebic [19], anti-inflammatory [20], hypoglycemic [21] and antimicrobial [22] activities. Similarly, cobalt complexes have demonstrated their cytotoxic activity against leukemia and lymphoma cell lines [23].

Keeping in view the attentiveness that pyrazine nucleus holds in the field of drug discovery and development, our continual search to discover newer antineoplastic agents directed us to aim this study to synthesize five transition metal complexes of well-known anti-mycobacterial agent, Pyrazinamide and perform their physical and spectroscopic characterization through H-NMR, FTIR, PXRD and

*To whom all correspondence should be addressed.

SEM and evaluate the cytotoxic activity of these complexes against human astrocytoma SNB-19, human Dukes' type C colorectal adenocarcinoma HCT-15, human Dukes' type D colorectal adenocarcinoma COLO-205 and human cervix carcinoma KB-3-1 cancer cell lines.

Experimental

Materials

Reference drug pyrazinamide (PZ) was obtained as a gift from Wyeth Pakistan Ltd. Karachi. The chlorides of iron(II), iron(III), manganese(II), cobalt(II) and copper(II) were all obtained from Sigma Aldrich and used without further purification. Solvents methanol (Sigma Aldrich) and water were freshly distilled just prior to use. Dulbecco's modified Eagle's Medium (DMEM), fetal bovine serum (FBS), penicillin/streptomycin and trypsin 0.25% were purchased from Hyclone (GE Healthcare Life Science, Pittsburgh, PA). Phosphate buffered saline (PBS) was purchased from Invitrogen GIBCO (Grand Island, NY). Dimethyl sulfoxide (DMSO) and 3-(4,5-dimethylthiazole-2-yl)-2,5-biphenyl tetrazolium bromide (MTT) were purchased from Sigma Chemical Co (St. Louis, USA).

Preparation of Complexes (PZ)

A 20 mL portions of PZ solutions (0.1 M, in methanol) were added in five different round bottom flasks containing different metal chloride. The resulting mixtures were kept stirring for few minutes at room temperature followed by refluxing on a water bath at 80°C for 3 to 4 h. The solid materials thus formed were filtered using Whatman filter paper and washed by hot methanol to furnish metal complexes of PZ.

Characterizations

The FTIR spectra were noted in KBr pellets using Shimadzu Prestige-21 spectrophotometer in the range of 4000-400 cm^{-1} . The $^1\text{H-NMR}$ spectra of PZ and its metal complexes were recorded in DMSO- d_6 on an Advance AV-400 and 500 MHz spectrometer. Morphological studies were performed on a Scanning Electron Microscope, Jeol Japan model no. JSM6380A with auto-coater JEOL JAPAN model no. JFC1500. X-ray diffraction (XRD) data were obtained at D8 Advance XRD, Bruker, UV-Visible, elemental and physico chemical analysis are reported in earlier paper [24].

Cell Lines and Cell Culture

The human astrocytoma SNB-19, human Dukes' type C colorectal adenocarcinoma HCT-15,

human Dukes' type D colorectal adenocarcinoma COLO-205, and human epidermoid carcinoma KB-3-1 cell lines were purchased from the American Type Culture Collection (ATCC, Manassas, VA). All cell lines were cultured at 37°C, 5% CO_2 with Dulbecco's modified Eagle's medium (DMEM), supplemented with 10% heat-inactivated FBS and 1% of 100 times diluted 10,000 IU/ml of penicillin-10,000 $\mu\text{g/ml}$ of streptomycin.

Cytotoxicity Assay

The cytotoxicity of the PZ and five PZ metal complexes to cultured cancer cells was determined by a modified MTT [3-(4,5-Dimethylthiazol-2-yl)-2,5-Diphenyltetrazolium Bromide] colorimetric assay. The assay assesses cell viability by detecting the formazan product formed from the reduction of yellow MTT by mitochondrial succinate dehydrogenase of metabolically active cells [25]. Cells were seeded in 96-well plates at a density of 5000 cells/well. After 24 h of incubation, various concentrations of the tested compounds were added respectively to the cells. After incubation for 72 h, MTT reagent (4 mg/mL) was added and the plates were incubated at 37 °C for 4 h. The supernatant was removed and 100 μl of DMSO were added to dissolve the formazan crystals. The plates were well shaken for 5 min, and the absorbance was determined at 570 nm by the accuSkan™ GO UV/Vis Microplate Spectrophotometer (Fisher Sci., Fair Lawn, NJ). The IC_{50} (concentration that inhibited the survival of cells by 50%) values were calculated to represent the cytotoxicity of the compounds.

Result and Discussion

FTIR Spectra

The aromatic skeleton of pyrazine in the PZ molecule containing two nitrogen did not participate in coordination because the absorption bands in the PZ spectrum were displayed in the same region with same intensities as were found its corresponding complexes, confirming non-participation of both ring nitrogen in the formation of coordinate covalent bond without the metal salts used during the synthesis of complexes reported in this study. The only two atoms of pyrazinamide were available to donate their lone pair to the metal ion for coordination; one is the oxygen of carbonyl and other nitrogen of amino group.

Hence for the determination of the coordination mode and geometry of the complexes under study the spectra were compared with that of ligand. IR data of Fe(II) and (III) PZ reported in earlier publication and IR data of Co(II)-PZ, Cu(II)-

PZ and Mn(II)-PZ are reported here with pure ligand in Table-1. The FTIR clearly showed no appreciable changes in the intensities of the absorption bands of the ring Nitrogen before and after complexation. This implied that the ring nitrogens did not take part in the complexation. On the other hand, no appreciable changes are observed in amino group vibrational wavenumbers which suggests that the amino nitrogen is likely to be not involved in coordination. From the appreciable shift of the wavenumber of the carbonyl vibration, we concluded that the coordination occurs through the oxygen of the carbonyl group. Similar findings for the complexes of PZ are reported by several researchers [26].

Table-1: FTIR data table of PZ and its metal complexes.

Peak Assign.	PZ	Cu(II)-PZ	Mn(II)-PZ	Co(II)-PZ
Frequency (cm ⁻¹)				
C=O	1686	1709	1709	1709
*N-H	3437	3437	3439	3442
**N-H	3140	3142	3138	3136
**Ring C-C	1506	1506	1508	1508
*Ring C-C	1604	-	1583	1583
**Ring C=N	1379	1383	1381	1381
*Ring C=N	1437	1437	1437	1435

* Asymmetric Stretching and ** Symmetric Stretching

¹H-NMR Spectra

The ¹H-NMR spectra of all complexes exhibited broad peaks as observed in the spectrum of PZ like splitting pattern which is more or less same, similarly their integration were also matched upon comparison with free PZ spectrum.

The closely matched peaks showed two doublets at 9.17 and 8.84 ppm of aromatic pyrazine ring in free PZ & its corresponding complexes having the integration of two protons each. Whereas broad two doublets at 7.84 and 8.23 of amide functional group were observed in the spectra of complexes but these peaks were found sharp doublet in PZ molecule.

The changes appeared in shape of peaks also provide a supportive conclusion towards the conversion of PZ into its corresponding metal complexes in Fig. 1.

X-Ray Diffraction

The X-ray diffraction technique was used to explore the morphology and solid state interaction between the pure PZ and its metal complexes. The resulting powder X-ray diffractograms are shown in Fig. 2 where prominent diffraction peaks in the range of 2θ = 10–60° is evident. Earlier findings suggest

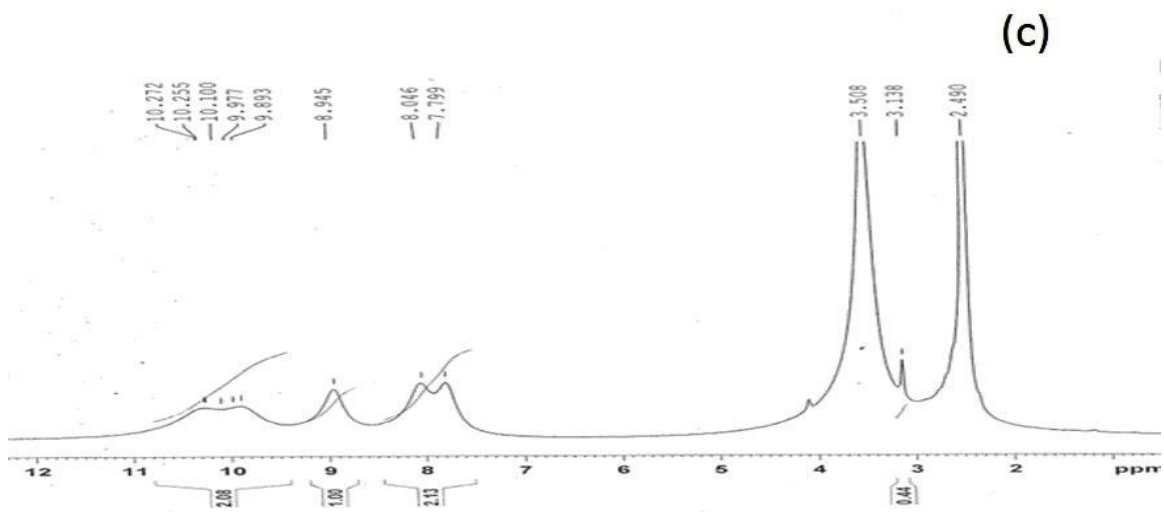
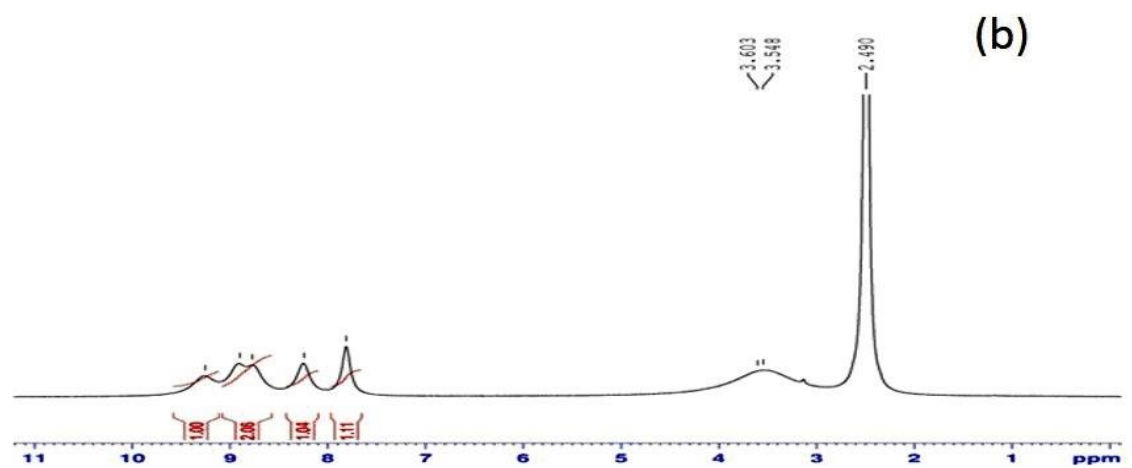
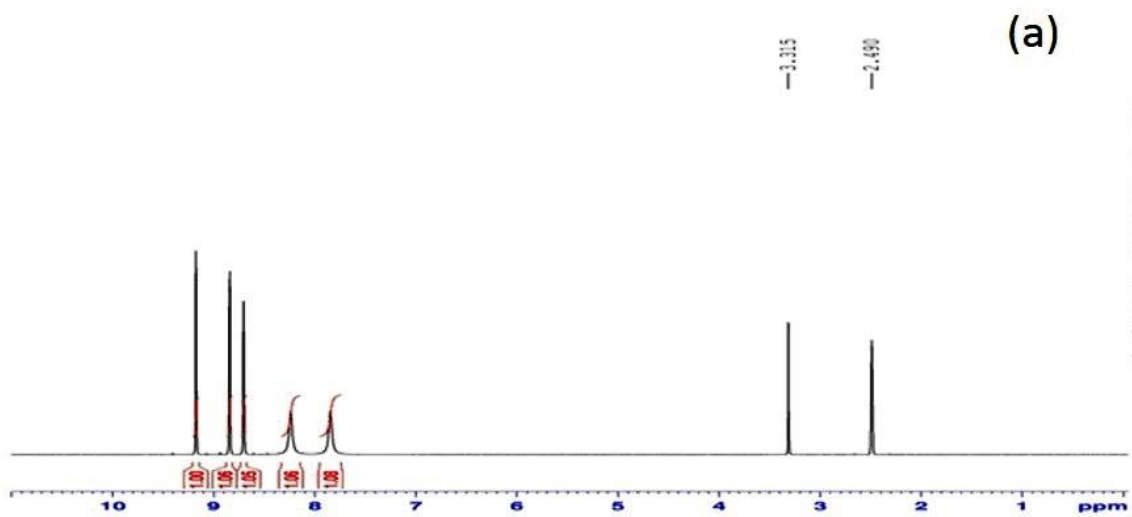
that PZ form planar rectangular plates or ribbons like crystals with a tendency of stacking due to hydrogen bonding. In case of pure PZ (Fig. 2a) the presence of peaks at different positions and relative intensities in PXRD diffraction patterns suggest the crystalline form of the drug. The characteristic diffraction peaks at 2θ values of around 14.0°; 15.7°; 17.8°; 23.7°; 27.8°; 36.0°; 38.5°; and 40.0° were obtained.

As reported by several researchers, PZ exists in four polymorphic forms (alpha, beta, gamma and delta) [25, 27, 28]. Marked changes in both peak positions and relative intensities in PXRD diffraction patterns of PZ are reported which are attributed to the polymorphic form and even, the processing conditions [29-31]. The X-ray scan of PZ (Fig. 2a) is in a fair agreement with the PXRD data presented by Gad et al [30] suggesting that the PZ sample used in this study is likely to be an alpha polymorph.

Fig. 2 (b to f) shows the X-ray diffractograms obtained for the PZ complexes with Mn(II), Cu(II), Co(II), Fe(II) and Fe(III) respectively. Remarkably, for all the transition metal complexes explored, PXRD diffraction patterns clearly revealed the appearance of diffraction peaks at various positions and intensities, suggesting the crystalline nature of these complexes. The appearance of crystallinity in the complexes is likely due to the inherent crystalline nature of the metals and ligand. Furthermore, in case of pristine PZ, the dominant diffraction peak was observed at 17.8° 2θ (Fig. 2a). The dominant peaks are observed at 2θ values of around 14.0° for all PZ metal complexes. The apparent shift in the dominant 2θ values to the lower energy side suggest that the structural phase changes occurred during the complexation process [32]. Compared to the diffractogram obtained for the pure ligand (Fig. 2a), different peak positions and relative intensities were observed for all the complexes which may likely be attributed to the formation of new structures as a result of complexation process [33]. In conclusion, PXRD data suggested crystalline nature for pure ligand and its corresponding complexes and this observation is well supported by morphological characterizations performed using Scanning Electron Microscopy.

Morphological Studies

To explore the morphological features of PZ and its various metal complexes, we employed scanning electron microscopy (SEM) which is considered to be a powerful tool to explore the surface morphologies and particle size distributions of a wide range of materials.



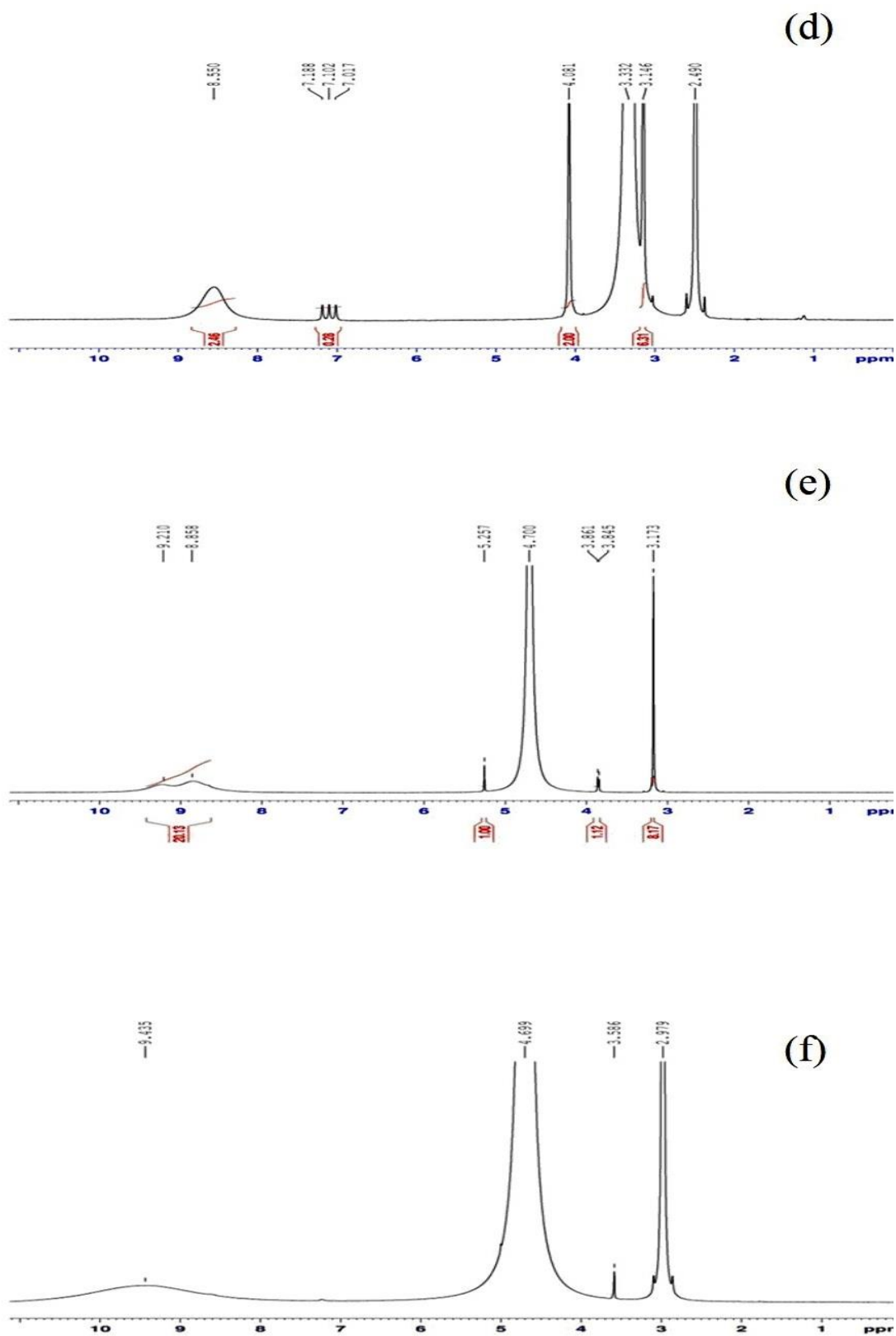


Fig. 1: $^1\text{H-NMR}$ spectra of (a) PZ, (b) Mn(II)-PZ , (c) Co(II)-PZ , (d) Cu(II)-PZ , (e) Fe(III)-PZ and (f) Fe(II)-PZ .

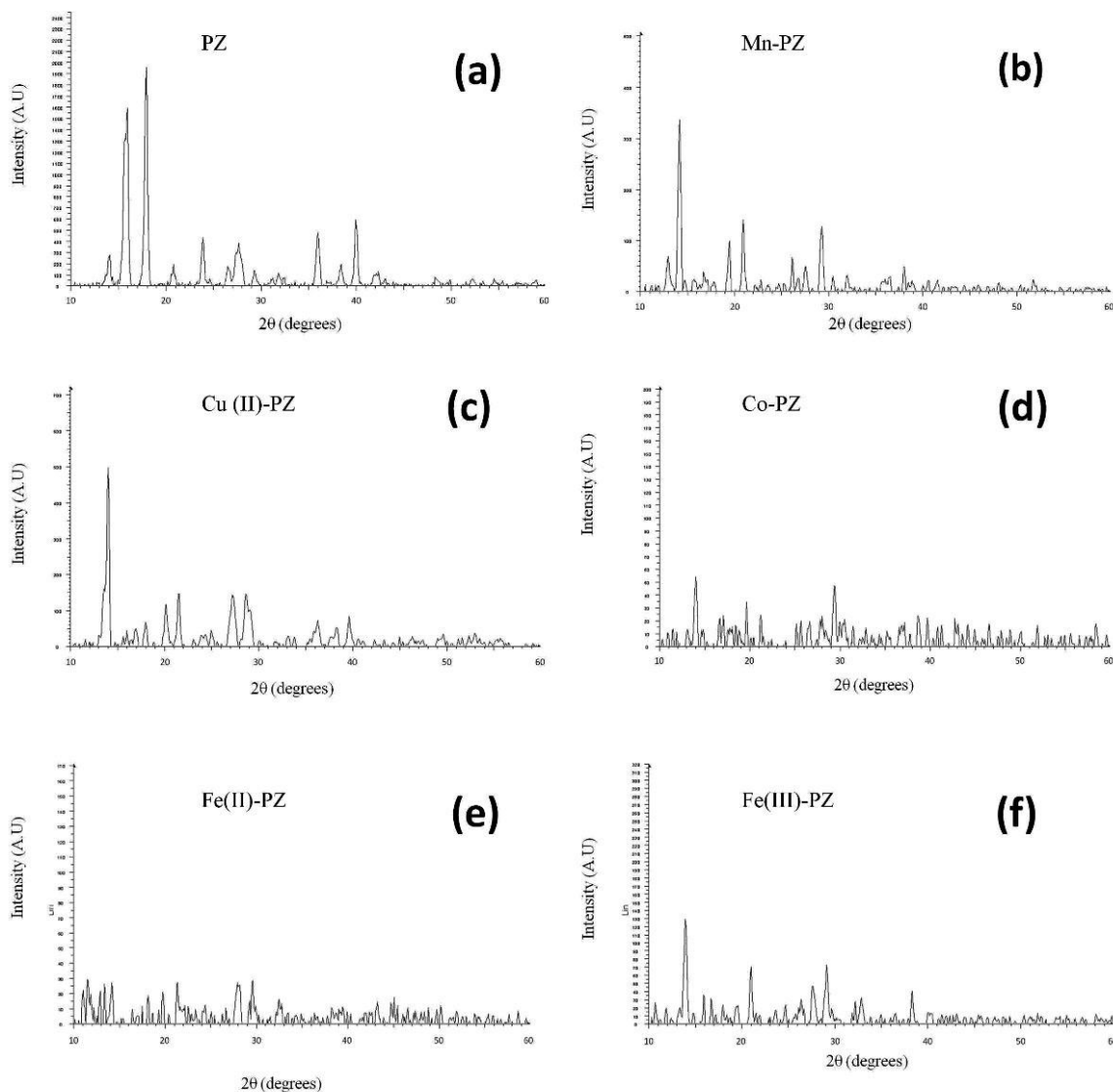


Fig. 2: X-ray diffractograms of pristine PZ (a), Mn-PZ (b), Cu-PZ (c), Co-PZ (d), Co-PZ (E), Fe (II)-PZ (F) and Fe (III)-PZ.

As shown in Fig. 3, scanning electron microscopy reveals some interesting morphological features for pristine PZ particles. Remarkably, the drug appeared to be composed of layered structure arranged uniformly in one direction. PZ is known to form planar rectangular plates or ribbons like crystals with a tendency of stacking due to hydrogen bonding [27, 34-36]. This peculiar morphology of PZ can be explained on the basis of inherent rigidity of its molecules which do not allow conformational polymorphism. However, four packing polymorphs, (α , β , γ , δ) exist due to different possibilities of intermolecular hydrogen bonding [31, 35]. The α polymorph is the most stable in which molecules are linked in centrosymmetric planar dimers that aggregate to form planar rectangular rods or ribbons which aggregate due to C-H...N interactions.

Fig. 4a and 4b show the morphologies of the Fe(II)-PZ and Co(II)-PZ complexes. In both the cases, an abrupt change in the morphological features was evident. Though the particle still exhibit anisotropic, rod-shaped crystals, but the features are not sharp compared to the pristine ligand (Fig. 3). A marked reduction in size is also visible whereas the size distribution is quite broad. This abrupt change in morphology is likely caused by the chelating of PZ molecules with the metals. The micrographs of both the complexes revealed a uniform matrix which suggest that the materials are likely to be in homogeneous phase and the drug uniformly dispersed at the molecular level [37, 38].

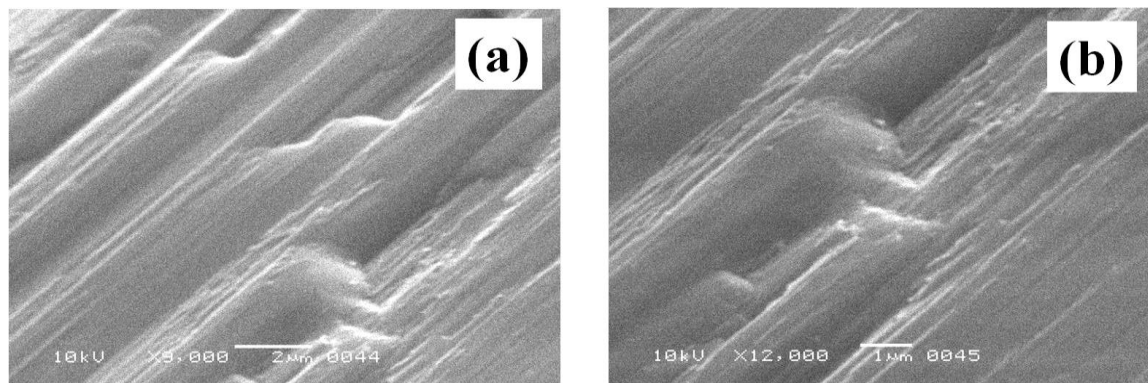


Fig. 3: Scanning Electron Micrographs of PZ at (a) lower and (b) higher magnifications.

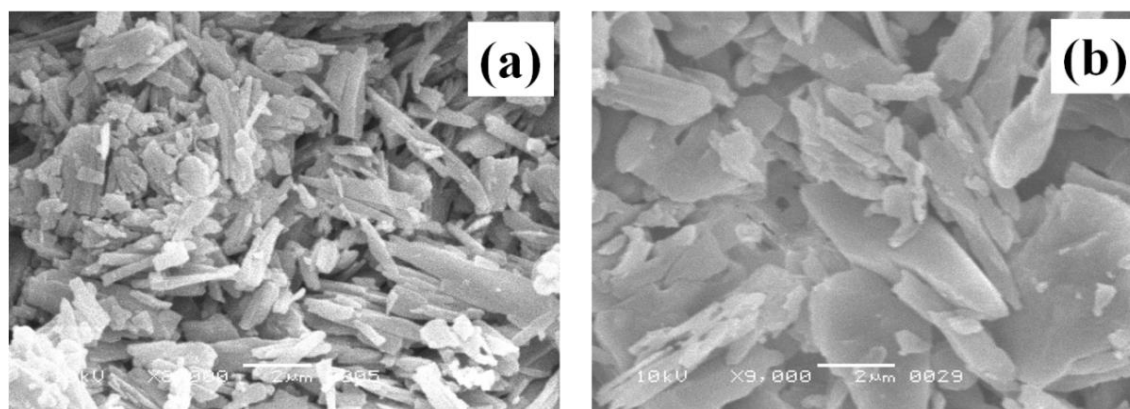


Fig. 4: SEM of (a) Fe(II)-PZ and (b) Co(II)-PZ complexes.

Fig. 5 shows the morphologies of the Cu(II)-PZ (Fig. 5a and b) and Fe(III)-PZ (Fig. 5c and d) complexes. Compared to what was observed for pristine PZ (Fig. 3), an abrupt change in the morphological features is evident for both the cases. The SEM images of Cu(II)-PZ (Fig. 5a and b) revealed that the sample composed of aggregates of small rod-like particles which resulted in the formation of flowers-like structures. Interestingly, SEM micrographs for Fe(III)-PZ also revealed flowers-like morphology composed of aggregation of small platelets (Fig. 5c and d). It is likely that these flower-like architectures are generated by the self-assembly of individual rods and platelets during the growth of the crystals [39, 40]. The formation of organic-inorganic hybrid flower-like morphologies for the coordination complexes of Cu(II) and Fe(III) ions with ligands is extensively studied in literature [39, 41]. It was proposed that the drug-metal complex act as locus for nucleation and grow to form rods and flaks which in turn undergo self-assembly to form three dimensional microspheres likely to minimize the high surface energy [42, 43].

The morphology Mn(II)-PZ complex particles is depicted in Fig. 6 (a and b). The complex

appeared as clusters of thin rectangular rods or needle-shaped crystals. The length of the rods appeared to be of several microns whereas the width appeared to be around 1.5 micron. The thickness was in the submicron range, resulting in a considerable high aspect ratio. Compared to pure PZ (Fig. 3), the change in morphology is quite appreciable and is likely attributed to the complex formation and a consequent loss of intermolecular C-H...N interactions resulting in an exfoliated morphology.

Cytotoxicity Assay

In order to understand the cytotoxic effects of pyrazinamide (PZ) and its derivatives, an MTT assay was carried out. As shown in Fig. 7, Mn(II)-PZ complex had low cytotoxic effect, with similar IC_{50} values (mean \pm standard deviation) $86.78 \pm 9.24 \mu\text{M}$. IC_{50} values of the PZ and its metal complexes on the cancer cell lines are summarized in Table-2. Cellular effects of these compounds were determined on four cancer cell lines. The compounds showed a significantly higher IC_{50} values ($>100 \mu\text{M}$) and are thus non- or low-toxic on these cell lines. These results indicated that these compounds have less potential of being anti-cancer drug candidates [44, 45].

Table-2: Cytotoxicity of MA Series on Four Human Cancer Cell Lines.

Compound	IC ₅₀ ± STD (μM)			
	SNB-19	HCT-15	COLO-205	KB-3-1
PZ	>100	>100	>100	>100
Fe(II)-PZ	>100	>100	>100	>100
Fe(III)-PZ	>100	>100	>100	>100
Cu(II)-PZ	>100	>100	>100	>100
Co(II)-PZ	>100	>100	>100	>100
Mn(II)-PZ	>100	>100	>100	86.78±9.24

Data represents the mean IC₅₀ values for each cell line ± SD obtained from three independent sets of experiments

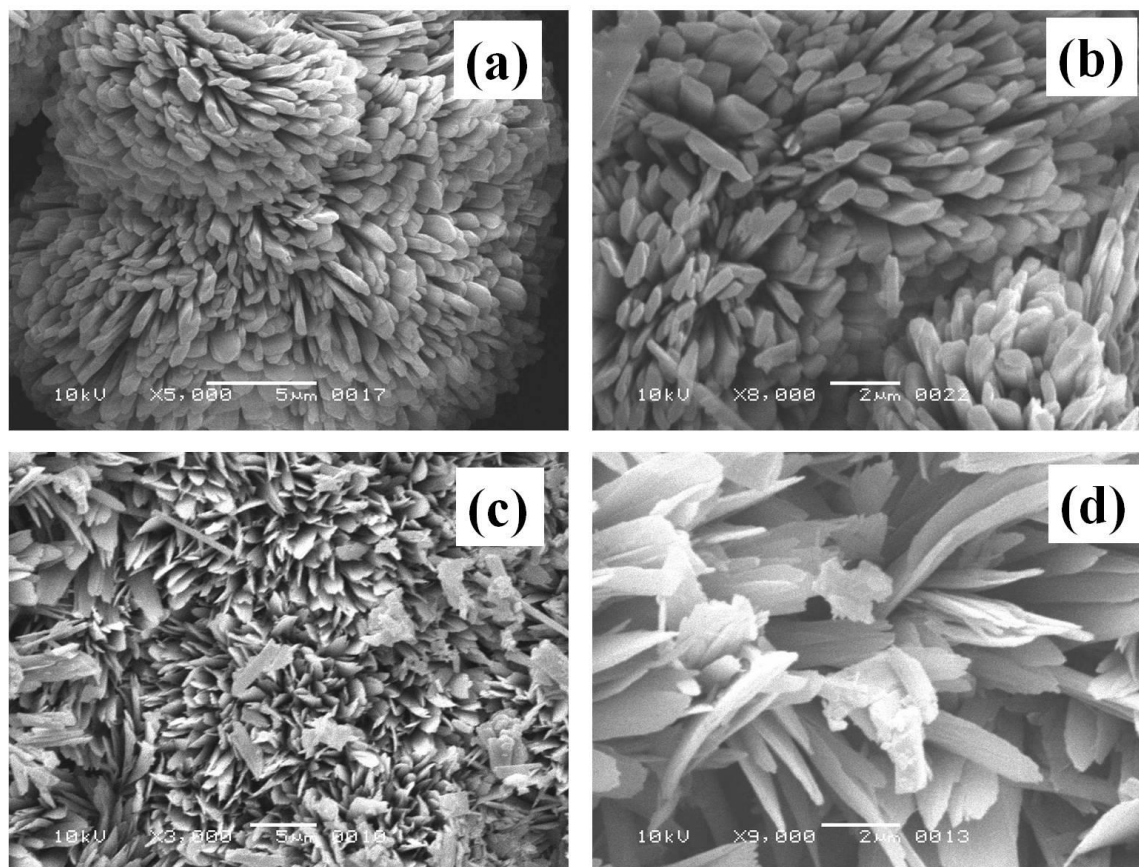


Fig. 5: SEM of (a and b) Cu(II)-PZ and (c and d) Fe (III)-PZ complexes.

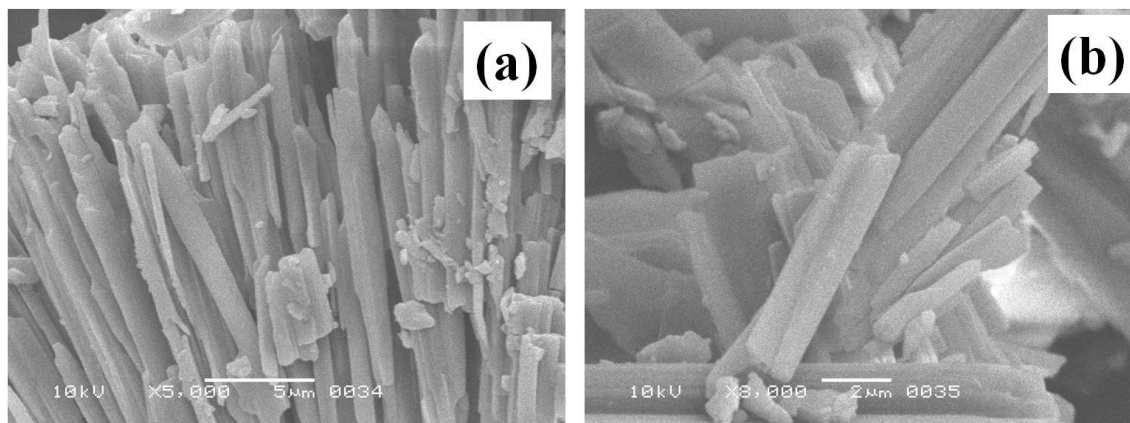


Fig. 6: SEM of Mn (II)-PZ complex particles at (a) lower and (b) higher magnifications.

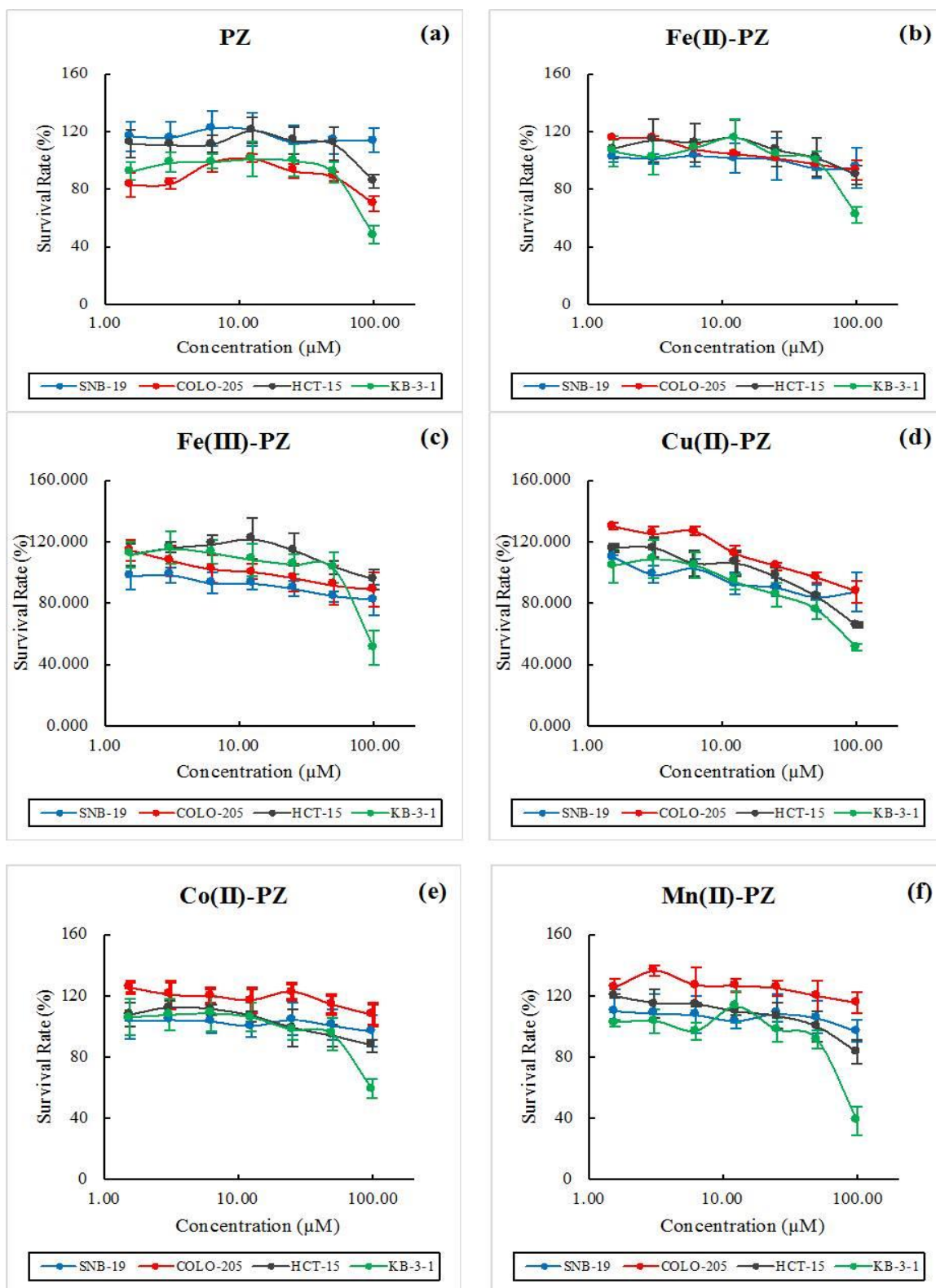


Fig. 7: The cytotoxicity of (a) PZ and five PZ metal complexes (b) Fe(II)-PZ, (c) Fe(III)-PZ, (d) Cu(II)-PZ, (e) Co(II)-PZ and (f) Mn(II)-PZ, against four human cancer cell lines SNB-19, COLO-205, HCT-15 and KB-3-1. Survival rate was determined by MTT assay. The mean \pm SD were calculated from three independent experiments.

Conclusion

We have presented the morphology and spectroscopic characterization of copper, cobalt, ferric, ferrous and manganese complexes of pyrazinamide. Spectroscopic characterizations revealed some interesting facts about the conversion of pure drug into its respective metal complexes. It was found that only the oxygen of carbonyl was involved in the coordination with the metal ions. Morphological characterization revealed that compared to the pristine ligand (pyrazinamide), the complexation results in marked changes in the morphology, however the drug was found to be uniformly dispersed.

The X-ray diffraction technique was used to explore the morphology and solid state interaction between the pure PZ and its metal complexes. As reported by several researchers, PZ exists in four polymorphic forms (alpha, beta, gamma and delta). Remarkably, for all the transition metal complexes explored, XRD diffraction patterns clearly revealed the appearance of diffraction peaks at various positions and intensities, suggesting the crystalline nature of these complexes. In conclusion, XRD data suggested crystalline nature for pure ligand and its corresponding complexes and this observation is well supported by morphological characterizations performed using Scanning Electron Microscopy. Unfortunately, the results of Cytotoxicity Assay indicated that these complexes have less potential to be used as anti-cancer drug candidates.

References

1. P. B. Miniyar, P. R. Murumkar, P. S. Patil, M. A. Barmade and K. G. Bothara, Unequivocal role of pyrazine ring in medicinally important compounds: A review, *Mini. Rev. Med. Chem*, **13**, 1607 (2013).
2. J. Hong, Y. Zhang, S. Lai, A. Lv, Q. Su, Y. Dong, Z. Zhou, W. Tang, J. Zhao and L. Cui, Effects of metformin versus glipizide on cardiovascular outcomes in patients with type 2 diabetes and coronary artery disease, *Diabetes care*, **36**, 1304 (2013).
3. A. C. Pinheiro and M. V. N. de Souza, The Relevance of New Drug Combinations for Modern Tuberculosis Treatment-A Patent Perspective, *Recent Pat Antiinfect Drug Discov*, **8**, 130 (2013).
4. N. Akuta, F. Suzuki, T. Fukushima, Y. Kawamura, H. Sezaki, Y. Suzuki, T. Hosaka, M. Kobayashi, T. Hara and M. Kobayashi, Prediction of treatment efficacy and telaprevir-resistant variants after triple therapy in patients infected with hepatitis C virus genotype 1, *J. Clin. Microbiol*, **51**, 2862 (2013).
5. S. G. Kang, W. H. Lee, Y. H. Lee, Y. S. Lee and S. G. Kim, Hypoxia-inducible factor-1 α inhibition by a pyrrolopyrazine metabolite of Oltipraz as a consequence of microRNAs 199a-5p and 20a induction, *Carcinogenesis*, **33**, 661 (2012).
6. A. B. Benson, Oltipraz: a laboratory and clinical review, *J. Cell. Biochem*, **53**, 278 (1993).
7. B. Piperdi, Y.-H. Ling, L. Liebes, F. Muggia and R. Perez-Soler, Bortezomib: understanding the mechanism of action, *Mol. Cancer Ther*, **10**, 2029 (2011).
8. A. Paramore and S. Frantz, Bortezomib, *Nat. Rev. Drug Discov*, **2**, 611 (2003).
9. S. A. Barnett and N. R. Champness, Structural diversity of building-blocks in coordination framework synthesis—combining M (NO₃)₂ junctions and bipyridyl ligands, *Coord Chem Rev*, **246**, 145 (2003).
10. W. K. Chan, Metal containing polymers with heterocyclic rigid main chains, *Coord Chem Rev*, **251**, 2104 (2007).
11. O. Kahn, Magnetism of heterobimetallics: toward molecular-based magnets, *Adv Inorg Chem*, **43**, 179 (1995).
12. R. L. LaDuca, Aliphatic and aromatic carboxylate divalent metal coordination polymers incorporating the kinked and hydrogen-bonding capable tethering ligand 4, 4'-dipyridylamine, *Coord Chem Rev*, **253**, 1759 (2009).
13. A. Morsali and M. Y. Masoomi, Structures and properties of mercury (II) coordination polymers, *Coord Chem Rev*, **253**, 1882 (2009).
14. A. Y. Robin and K. M. Fromm, Coordination polymer networks with O- and N-donors: What they are, why and how they are made, *Coord Chem Rev s*, **250**, 2127 (2006).
15. S. Akyuz, The FT-IR spectra of pyrazinamide complexes of transition metal (II) tetracyanonickelate, *J Mol Struct*, **651**, 541 (2003).
16. A. M. Beatty, Hydrogen bonded networks of coordination complexes, *Cryst Eng Comm*, **3**, 243 (2001).
17. A. M. Beatty, Open-framework coordination complexes from hydrogen-bonded networks: toward host/guest complexes, *Coord Chem Rev*, **246**, 131 (2003).
18. F. Prins, E. Pasca, L. J. de Jongh, H. Kooijman, A. L. Spek and S. Tanase, Long-Range Magnetic Ordering in a TbIII–MoV Cyanido-Bridged

- Quasi-One-Dimensional Complex, *Angew. Chem. Int. Ed.*, **46**, 6081 (2007).
19. Z. Qin, M. C. Jennings and R. J. Puddephatt, Self-assembly of polymer and sheet structures from palladium (II) complexes by hydrogen bonding between carboxamide substituents, *Inorg. Chem.*, **40**, 6220 (2001).
 20. K. Rainsford, K. Brune and M. Whitehouse, Aspirin and related drugs: Their actions and uses, *Agents and Actions [Suppl 1]. Birkhäuser, Basel Stuttgart*, **7** (1977).
 21. N. Yasumatsu, Y. Yoshikawa, Y. Adachi and H. Sakurai, Antidiabetic copper (II)-picolinate: impact of the first transition metal in the metallopicolinate complexes, *Bioorg. Med. Chem.*, **15**, 4917 (2007).
 22. T. Suksrichavalit, S. Prachayasittikul, C. Nantasenamat, C. Isarankura-Na-Ayudhya and V. Prachayasittikul, Copper complexes of pyridine derivatives with superoxide scavenging and antimicrobial activities, *Eur. J. Med. Chem.*, **44**, 3259 (2009).
 23. I. Ott, B. Kircher and R. Gust, Investigations on the effects of cobalt-alkyne complexes on leukemia and lymphoma cells: cytotoxicity and cellular uptake, *J. Inorg. Biochem.*, **98**, 485 (2004).
 24. A. Mohsin, Q. Shah Ali Ul, Shahid, Faiza; A. M. Saeed; M., Majid, Synthesis, characterization and enzyme inhibitory activity of new pyrazinamide iron complexes, *Pak. J. Pharm. Sci.* **30**, 825-831. (2017)
 25. J. Carmichael, W. G. DeGraff, A. F. Gazdar, J. D. Minna and J. B. Mitchell, Evaluation of a tetrazolium-based semiautomated colorimetric assay: assessment of chemosensitivity testing, *Cancer Res.*, **47**, 936 (1987).
 26. Akyuz S. *The FT-IR spectra of pyrazinamide complexes of transition metal (II) tetracyanonickelate. Journal of molecular structure.* 2003 Jun 1;651:541-5."
 27. R. A. Castro, T. M. Maria, A. O. Évora, J. C. Feiteira, M. R. Silva, A. M. Beja, J. Canotilho and M. E. S. Eusébio, A new insight into pyrazinamide polymorphic forms and their thermodynamic relationships, *Cryst. Growth Des.*, **10**, 274 (2009).
 28. S. T. Cherukuvada, Ranjit; Nangia, Ashwini Polymorphs, Pyrazinamide, Pyrazinamide polymorphs: Relative Stability and Vibrational Spectroscopy, *Cryst. Growth Des.*, **10**, 3931 (2010).
 29. X. Tan, K. Wang, S. Li, H. Yuan, T. Yan, J. Liu, K. Yang, B. Liu, G. Zou and B. Zou, Exploration of the pyrazinamide polymorphism at high pressure, *J. Phys. Chem. B*, **116**, 14441 (2012).
 30. S. Gad, Effect of a particle engineering process on polymorphic transition of pyrazinamide, *J Pharm Pharm Sci.*, **7**, 581 (2014).
 31. Y. Takaki, Y. t. Sasada and T. Watanabe, The crystal structure of α -pyrazinamide, *Acta Crystallogr.*, **13**, 693 (1960).
 32. L. N. Suvarapu and S.-O. Baek, Synthesis and Characterization of 4-Benzyloxybenzaldehyde-4-methyl-3-thiosemicarbazone (Containing Sulphur and Nitrogen Donor Atoms) and Its Cd (II) Complex, *Metals*, **5**, 2266 (2015).
 33. F. A. Al-Saif and M. S. Refat, Synthesis, spectroscopic, and thermal investigation of transition and non-transition complexes of metformin as potential insulin-mimetic agents, *J. Therm. Anal. Calorim.*, **111**, 2079 (2013).
 34. A. Borba, M. Albrecht, A. Gómez-Zavaglia, M. A. Suhm and R. Fausto, Low temperature infrared spectroscopy study of pyrazinamide: from the isolated monomer to the stable low temperature crystalline phase, *J. Phys. Chem. A*, **114**, 151 (2009).
 35. V. Chiş, A. Pirnau, T. Jurca, M. Vasilescu, S. Simon, O. Cozar and L. David, Experimental and DFT study of pyrazinamide, *Chem Phys*, **316**, 153 (2005).
 36. D.-D. Pham, E. Fattal, N. Ghermani, N. Guiblin and N. Tsapis, Formulation of pyrazinamide-loaded large porous particles for the pulmonary route: avoiding crystal growth using excipients, *Int. J. Pharm.*, **454**, 668 (2013).
 37. J. Joseph and G. B. Janaki, Synthesis, structural characterization and biological studies of copper complexes with 2-aminobenzothiazole derivatives, *J Mol Struct.*, **1063**, 160 (2014).
 38. S. Malik and S. Wankhede, Synthesis, Characterization and Biological Activity of Fe-III and Co-II Complexes derived from 4-Chloro-2-[(2-Furanylmethyl)-Amino]-5 Sulfamoylbenzoic Acid, *Int J Appl Biol Pharm.*, **6**, 205 (2015).
 39. E. Moretti, L. Storaro, A. Talon, P. Riello, A. I. Molina and E. Rodríguez-Castellón, 3-D flower like Ce-Zr-Cu mixed oxide systems in the CO preferential oxidation (CO-PROX): Effect of catalyst composition, *Appl. Catal., B*, **168**, 385 (2015).
 40. Y. Zou, Y. Li, X. Lian and D. An, Preparation and Characterization of Flower-shaped CuO Nanostructures by Complex Precipitation Method, *J. Mater. Sci.*, **3**, 44 (2014).
 41. X. Huang, J. Guan, Z. Xiao, G. Tong, F. Mou and X. a. Fan, Flower-like porous hematite nanoarchitectures achieved by complexation-mediated oxidation-hydrolysis reaction, *J. Colloid Interface Sci.*, **357**, 36 (2011).

42. T. Huang, Sun, Y. F. et.al, Hierarchical hollow Fe₂O₃ micro-flowers composed of porous nanosheets as high performance anodes for lithium-ion batteries, *RSC Adv.* **3**, 20639 (2013).
43. T. R. Penki, S. Shivakumara, M. Minakshi and N. Munichandraiah, Porous Flower-like α -Fe₂O₃ Nanostructure: A High Performance Anode Material for Lithium-ion Batteries, *Electrochimica Acta*, **167**, 330 (2015).
44. D. S. Wang, G. H. Rizwani, H. Q. Guo, M. Ahmed, M. Ahmed, S. Z. Hassan, A. Hassan, Z. S. Chen and R. H. Xu, Annona squamosa Linn: Cytotoxic activity found in leaf extract against human tumor cell lines, *Pak J Pharm Sci*, **27**, 1559 (2014).
45. H. Guo, D. S. Wang, G. H. Rizwani, M. Ahmed, M. Ahmed, A. Hassan, R. H. Xu, N. Mansoor, A. K. Tiwari and Z. S. Chen, Antineoplastic activity of Holoptelea integrifolia (Roxb.) Planch bark extracts (in vitro), *Pak J Pharm Sci*, **26**, 1151 (2013).